

Proposal of a Method for Measuring Gas Flow in a Heating Furnace: A Simulation Study

Marcel Pástor¹, Milan Durdán², Ján Kačur^{2*}, Marek Laciak², Patrik Flegner²

¹ Technical University of Košice, Faculty FMMR, Institute of Metallurgy, Letná 9, 042 00 Košice, Slovak Republic

² Technical University of Košice, Faculty BERG, Institute of Control and Informatization of Production Processes, Némcovej 3, 042 00 Košice, Slovak Republic

* Corresponding author's e-mail: jan.kacur@tuke.sk

ABSTRACT

Metallurgy, as one of the oldest industries, is currently experiencing a technological boom in an effort to increase production efficiency with the least possible impact on the environment. Modeling methods make it possible to design and simulate a technological process or technological equipment for conditions that take into account the above-mentioned aspects. For this reason, the article focuses on the use of simulation modeling using accessible computer technologies in order to improve the operation of heating aggregates with the metal-bearing batch, such as a continuous heating furnace. The paper describes the methodology for modeling the flow of flue gases in the working space of a gas heating furnace, which results in their enthalpy representation. A simulation study was performed for a gas-fired furnace used to heat gates. Three case studies were simulated with set values of on and off burners and fuel flow to them. The effect of these parameters on the total amount of recirculated flue gas was investigated. The results showed that the fuel flow regulation to the burners at the material inlet into the furnace had a higher effect on the overall recirculation than the switching on and off the burners on the furnace's outlet side. The results pointed to critical points on the inner shell of the furnace, which could be the most critically thermally stressed, for example, in the places of the collision of opposing flue gas flows.

Keywords: gas flows, burners, modeling, simulation, flue gas, volume zones.

INTRODUCTION

Along with the development of new metallurgical technologies (e.g., the use of hydrogen and biomass), the innovation of existing technologies, such as technological heating equipment, is taking place in parallel. The aim of the innovation is to increase the quality of the final heated product while reducing consumption and maintaining the quality of the heating medium. One of the means to achieve these requirements is the methodology of mathematical and simulation modeling. This methodology is still evolving in order to apply it to selected technologies, not only in the field of metallurgy.

Hassan et al. [1] developed a model for predicting temperature within the load and the belt in the heat treatment of randomly distributed metal parts processed in multi-zone continuous

mesh-belt furnaces. This model counts with the convection and radiation heat transfer to the load and the belt where gas radiation is caused by the presence of CO₂ and/or H₂O gases in the furnace atmosphere. Experimental data obtained from two industrial facilities were used to model validation. There was a maximum difference of 12% between the prediction and measured data.

Honner et al. [2] described the possibilities of the measuring technique and computer modeling for the analysis of continuous reheating furnaces. Results are shown with a particular example of the calibration measurement of the pusher-type furnace. The definition of governing partial differential equations led to the model of computing which covers two relations: the first between the furnace thermocouples temperature and the furnace temperature distribution where average

disagreement was 53.5 K (i.e., between the measured and computed temperature), the second between the furnace temperature distribution and the billet temperature evolution where average difference 10.5 K was reached at the billet axis.

The modeling and simulation of the heat transfer process are of great importance from the perspective of the prediction and control of the final microstructure and properties of workpieces, which are processed in the heat treatment furnace. Kang et al. [3] dealt with mathematical modeling and computer simulation of heat transfer in loaded continuous heat treatment furnace. The heat transfer models (i.e., radiation, convection, and conduction model) are integrated with the furnace model (i.e., heat storage in load, heat storage in the furnace, shell cooling, heat loss from the walls and opening, etc.) to simulation the workpieces heat treatment processes. Optimization of workpiece loading and the thermal schedule is used to improve heat treatment quality and efficiency. The maximal difference between measured and calculated temperature is circa 100 °C. A three-dimensional numerical simulation of the transient heat transfer and turbulent fluid flow in a continuous industrial furnace (i.e., arc-welding electrode furnace) using FLUENT software is presented by Rad et al. [4]. The electrode geometry and material composition were simplified, and the electrode movement inside the furnace was avoided. The simulation accuracy was influenced by the movement of the electrodes, the existence of various modes of heat transfer, etc. The absolute relative difference below 2.7 % was obtained by comparing the load's temperature history to the experimental data. A three-dimensional mathematical model for a continuous annealing furnace is described by Fuyong [5]. This model is calculating the flow and temperature field of the furnace and the temperature of the stainless strip. The results showed that the radiation is the main heat transfer in this furnace by comparing the convection and radiation heat transfer coefficients. The maximum relative error was less than 4.4% by comparing the simulation results again measured temperature. Zhou et al. [6] deal with the modeling of the heating process realized in a horizontal annealing furnace, which is used for producing stainless steel. The proposed steady-state model allows determining the strip temperature in the heating section. The model was verified by experiments, where two measurement points monitoring the temperature of strip steel, the first one was in the

burning area, and the second one was at the exit of the heating section. The strip temperature difference between measured and calculated was at range 50 to 70 °C in the burning area and within 5 °C at the exit section.

Sahay and Kapur [7] proposed the scheduling algorithm linked with the process model for a continuous annealing furnace, where are bundles of steel rods annealed. The heat transfers and annealing kinetics were included in the process model. The variable hearth speed and constant hearth speed were examined in this paper. The results showed that the most efficient is charging the rods in ascending order of diameter. The constant hearth speed is the most efficient method for the short dispatch time, and the variable hearth speed method is the most efficient method for longer dispatch times. Zhang et al. [8] have described a state observer-based method. This method was using the out surface temperature and pressure of a scramjet combustor for the indirect online measurement of the inner wall temperature using. It was developed a mathematical model that describes the heat transfer by convection from gas to the combustor wall and the heat transfer by conduction inside the combustor wall. The proportional integral observer determined the relationship between the observed inner wall temperature and the measurable variables. The relative error was less than 5% at numerical simulation and maximal 20% at ground experiments. A process model for determining the heating cycles for bundles of packed rods in a continuous annealing furnace is described by Sahay and Krishnan [9]. This model determines the spatial and temporal behavior of temperature and hardness in the bundle of packed rods that are going through the furnace. The process model consists of two models, the first, the thermal conductivity model to obtain radial conduction within the packed bundle, and the second, a thermal model to capture heat transfer across the bundle. This model has been implemented in an industrial operation resulting in around 20% energy reduction and 15% productivity enhancement, despite small differences between experimental data and calculated data (i.e., temperature and hardness).

Continuous reheating furnaces are used in the steel industry to heat steel products, especially slabs, before its hot processing. Steinboeck et al. [10] described a feedback controller, which adjusting reference trajectories of furnace temperatures. This controller is based on a nonlinear

dynamic model that consists of the radiative heat transfer in the furnace and the conductive heat transfer within the slabs. The emulator of the inner control loop and the simulation environment using the validated mathematical model presented by Wild et al. [11] were used to test this controller. The results showed that almost all slabs reached their desired final temperature range (i.e., desired temperature ± 15 K). The analysis of the effects of the strip velocity, strip thickness and width, and also heating power produced by radiant tubes in terms of the continuous annealing furnace efficiency were performed by Hajaliakbari and Has-sanpour [12]. A mathematical model that consists of radiative and convection heat exchange was developed for computing total heat absorbed by the strip. The verification showed that the model predicts the strip temperature with an error of less than 5% by comparing results and experimental data. Goyheneche and Sacadura [13] describe an application of the zone method for determining an explicit matrix relation, which allows calculation of the total exchange areas in emitting, absorbing, and anisotropic scattering semi-transparent medium. Authors assume that the medium is bounded by the emitting, absorbing, and anisotropically reflecting walls. Subsequently, new formulations of direct exchange areas and indirect exchange areas have been proposed, which allow the computation of the exchange areas of complex elements like unstructured meshes and solving a nonstationary heat transfer problem. Hu et al. [14] describe a new heat transfer mathematical model of the hot-wall heat exchanger based on analytic solutions. The proposed model includes equations of the heat transfer by conduction and convection, which were adjusted for solving the problem. The deviations of heat flux 2.53%, 0.99%, 2.12%, and 1.96% were reached in the validation of this model under four conditions with literature values. Hu et al. [15] described the zone method developed for industrial steam cracking furnaces. This zone method was used for the firebox side, and the one-dimensional reactor model COILSIM1D (i.e., the commercial software tool) was used for the reactor side. The firebox model includes two models, i.e., the flow model and the combustion model used to calculate the radiation heat transfer. The results showed that relative error was in the range 0.65 to 4.05% at a comparison of the zone method simulation with CFD (i.e., computational fluid dynamics) simulation. A two-zone model to the prediction of knocking performance and NO emission

for a marine natural gas engine is described by Xiang et al. [16]. The flame propagation process in the form of the volume balance between two cylindrical zones with three boundary parameters (i.e., initial mass coefficient, the entrainment factor, and the Heider–Holhbaum factor) is the basic assumption of this paper. The results based on the change of boundary parameters also showed an influence of compression ratio and ignition angle on the probability knocking probability, knocking timing, and knocking intensity. Kreuzer and Werner [17] described the implementation of physical models for reheating processes in industrial furnaces as pusher-type and walking beam furnaces. The authors had an assumption dividing the furnaces into three zones as a convective, heating, and soaking zone. The heat transfers between furnace walls, flue gas, and the processed steel goods was computed by using the proposed cell model where a one-dimensional method was used for modeling the radiative heat transfer. The proposed models allow show time behaviors of slab temperature, heat flow at the top and bottom surface of the slab, and gas and wall temperature of top cells. A quasi-dimensional model for fast and accurate automated design of spark engines is described by Kaprielian et al. [18]. This model is based on a three-dimensional model created by adding a reacting zone near the walls to the two-dimensional model. Subsequently, a multi-zone model was created by dynamically adding new reacting zones at given crank-angle intervals. The results showed decreasing the relative error in sequence the two-dimensional model error, the three-dimensional model error (i.e., at full load conditions), and the N-dimensional model error (i.e., at partial load conditions).

A control-oriented two-zone thermodynamic model (i.e., reaction and unburned zones) to describe the thermal performance and combustion process of spark-ignition engines is proposed by Li and Zhu [19]. This chemical reaction based model is focused on the in-cylinder dynamic process between exhaust valve opening and intake valve closing and includes heat and mass transfer between zones for reaching a smooth combustion process. The simulation results based on in-cylinder pressure relative error within 5.3% confirmed that the proposed model is can used for model-based combustion control and prediction of the heat release rate, mass-fraction-burned, and in-cylinder pressure in real-time. Oba et al. [20] describe the simulation model of a tunnel kiln

consists models for determining energy distribution in the burning zone, the advection of gases inside the furnace, and the calculation of heat transfer by radiation between ceramic load and refractory walls. The authors have an assumption that the kiln consists of three main zones as pre-heating, furnace, and cooling. The results showed that it is possible to optimize energy efficiency and production of the kiln based on obtained simulation data as the characteristic firing curve of the kiln, temperature distribution in the load, walls, and gases, etc. Shiehnejadhesar et al. [21] proposed a hybrid gas-phase combustion model of biomass grate furnaces to the flame prediction. This model is a combination of FRK (i.e., finite rate kinetics) and EDC (i.e., eddy dissipation concept) models and is suitable for low and high turbulent combustion conditions. The results of the hybrid model showed good agreements with measurement data for prediction of flame, in which the reaction zones are out of the EDC validity range. A modified one zone model to design recommended fire protection in a fire compartment is described by Zhang and Usmani [22]. This model is in the form of a heat balance equation and included the heat sink effect of the steel members. Subsequently, it was discussed a localized fire model for calculation of the heat fluxes to structural members. This model was compared with the two-zone model (i.e., cool and hot zone), and the results showed that it is recommended for structural fire safety design in large enclosures. A mathematical model of biomass combustion and prediction of emission generation (i.e., NO_x and CO) is described by Lukáč et al. [23]. This model includes temperatures calculations, the stoichiometry of combustion, and regression equations of NO_x and CO. The model verification showed that the prediction of NO_x and CO in combustion devices is possible only if combustion process parameters can be measured and, in the case of NO, only for quick verification of the produced amount of nitrogen oxides.

The aim of the described methods is to increase the efficiency of the production of industrial aggregates, which is also related to the assessment of economic impact. Various methods are designed and implemented around the world to assess economic efficiency. An example is a study described by Drábikova and Škrabul'áková [24], where the methodology based on the k-means cluster method for reducing costs in different business and industrial areas is described. This methodology

is created by the implementation of graph models and algorithms. Cost-saving using graph theory is also discussed by Škrabul'áková and Grešová [25]. Specifically, modeling by a graph and graph coloring algorithm approach is applied. What is very convenient, the model suggested by the authors can be used for multiple areas and cases.

It can be seen from the presented articles that the idea of increasing the efficiency of production of industrial aggregates is still relevant. Models are described using stationary and non-stationary heat transfer knowledge in mentioned articles. These models aim to calculate the process temperature (i.e., the furnace atmosphere's temperature, furnace lining's temperature, processed material's temperature, etc.). It is essential in terms of the quality of the implemented technology. Low differences of temperatures (i.e., below 30 °C) between modeled (i.e., calculated) temperatures and measured temperatures are mostly achieved at the exit of the material from the furnace (e.g., Zhou et al. [6]), or in specific types of technology (e.g., Rad et al. [4]). More significant differences in temperatures (i.e., in the range of 30–100 °C) are found along the length of the furnace (e.g., Hassan et al. [1], Honner et al. [2], Kang et al. [3], etc.). These temperature differences have a negative effect on the quality of the final product because the technological temperature curve of the material processing is not achieved (i.e., required material structure change by temperature change). The heat transfer by radiation from the flue gas to the charge is influenced by the dissociation of the flue gas, which depends not only on the temperature but also on the furnace space's pressure conditions. Temperature differences of models along the furnace space length could be caused by the absence of the effect of dissociation and recirculation of flue gases. Including the flue gas recirculation process in the calculation, i.e., determining the flue gas flow in individual parts of the furnace would increase the balance calculations accuracy and thus reduce the differences of the calculated temperatures in the zone methods used (e.g., Goyheneche and Sacadura [13], Hu et al. [15], Xiang et al. [16], etc.).

In this article, the authors proposed a balance model of flue gas flows while maintaining a material balance that is closely related to the energy balance. This model is based on the geometry of the flue gas flow in the working space of heat generators, the result of which is their volume-zonal redistribution.

The results of volume-zonal redistribution are used for determining the most thermally stressed places that are important in terms of technological equipment life. The acquired knowledge can be used to optimize the structure of the furnace (e.g., changing the burners' location and their operating characteristics).

The proposed model can then be used as an input for the simulation apparatus for a more detailed calculation of temperatures in the furnace space and inside the heated material, where the result is to determine the overall energy efficiency of the device.

THE DESCRIPTION OF A MODELED HEATING FURNACE

Natural gas burners are located on the front walls of the furnace (see Fig. 1). The input to the burners on the inlet side is 1300 Nm³/h and on the outlet side, 559 Nm³/h. The inner diameter of the burners is 0.116 m. The combustion air (with an excess of 1.12) was heated by a central metal recuperator on temperature 280 °C. Flue gas extraction is provided by three openings in the furnace ceiling at a distance of one-third of the furnace length from the rear burner wall. They lead to a common exhaust pipe.

The main technical parameters of the furnace:

- batch – steel class: 10, 11, 12, 15,
- maximum loupe (i.e., heating slab bloom) length: 16200 mm,

- batch temperature: 350 to 725 °C,
- heating temperature: 950 to 1000 °C,
- maximum temperature in the working space of the furnace: 1050 °C,
- average furnace output: 150 to 180 loupe/h,
- furnace dimensions: length 17000 mm, width 8370 mm, height 1600 mm.

In the furnace, the thermocouples are located at a distance of 1850 mm from the sidewall and the front wall, respectively, 3210, 9510, and 14610 mm.

MODELING OF FLUE GAS FLOWS

The construction of the burner and the properties of the used fuel determine the aerodynamics of the flame. The modeling of the burner uses the analogy of the transmission mechanism between the behavior of the flame and the outflow of the gas stream. This transmission mechanism affects the properties of the environment into which the stream flows. In the conditions of industrial furnaces, the stream flows from the burner hole of a relatively small cross-section into the working space – here is distinguished the outflow of free stream, the limited (i.e., bounded) stream outflow respectively. The turbulent free stream flows into the environment with different densities and does curving. Due to the transverse pulsations, the mass of the stream exchanges with the surrounding environment. The weight of the stream increases, and its boundaries expand. Kinetic energy and thus the

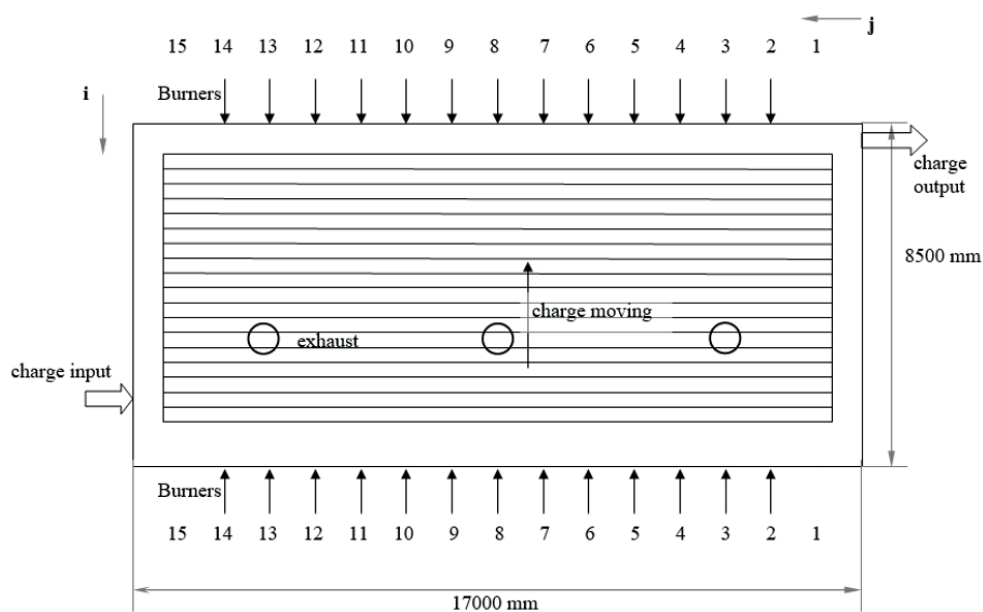


Fig. 1. Top view of a modeled furnace

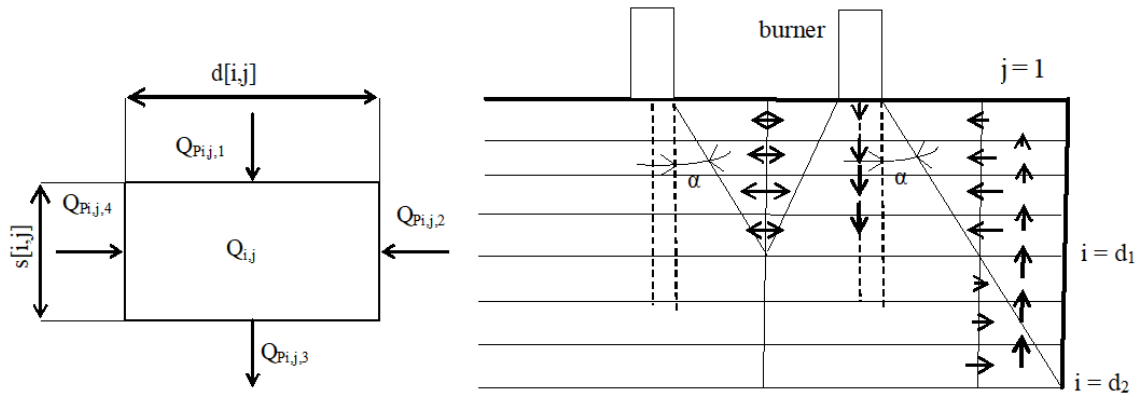


Fig. 2. The orientation of the flow in the zone and an example of a stream for the edge zones

stream speed gradually decreases, the momentum of the stream remains constant.

The model of the convection (i.e., jet stream model) was created based on the aerodynamic properties of a stationary turbulent flame. The result is the determination of volume flows through the individual surfaces of the volume zones of the combustion space.

In Figure 2 on the left is the orientation of the supplied and exhausting amounts of flue gas for the zone and the total amount in the zone $Q_{(i,j)}$, which is the sum of all quantities supplied (i.e., positive $Q_{(Pi,j,k)}$). On the right, the redistribution of the flow into individual volume zones is indicated.

Kirchhoff's law can be applied to flow rates through fictitious surface zones, delimiting volume zones (i.e., for $i = 1, \dots, m; j = 1, \dots, n$):

$$\sum_{k=1}^4 Q_p(i, j, k) = 0 \quad (1)$$

where: i, j are indexes of volume zone, k is the index of the surface, i.e., fictitious zone i of the j -th volume zone, and parameters m, n represent the total number of zones in the vertical and horizontal directions.

The number of volume zones can be chosen arbitrarily, for given transverse dimensions of the combustion space. Optimally, the proportional division corresponds to the maximum number of burners placed on the burner wall.

The length of the zone $d(i,j)$ must be greater than the diameter of the burner outlet d_h , for which the maximum outlet speed must be observed, which is determined by the type of the burnt fuel. The width of the zone $s(i,j)$ is proportional to the length of the initial flame section, where the flow velocity is the same over the entire width of the flame.

The following restrictions apply to flow rates through surface zones:

In the case of the real surface of the zone with the burner (i.e., for $j = 2, \dots, n - 1; i = 1, m; if i = 1 \Rightarrow k = 1; if i = m \Rightarrow k = 3$)

$$Q_p(i, j, k) = Q_0(i, j) \quad (2)$$

where $Q_0(i, j)$ is the amount of flue gas produced by each burner (m^3/s).

The amount of flue gas is determined by the type of fuel and the amount of oxidizing agent. In the case of a real wall surface (i.e., for $i = 1, \dots, m; j = 1, n; if j = 1 \Rightarrow k = 2; if j = n \Rightarrow k = 4$)

$$Q_p(i, j, k) = 0 \quad (3)$$

Radius of beam (m) on boundary of i -th zone (i.e., for $i = 1, \dots, m; j = 2, \dots, n - 1$):

$$r(i, j) = (s(1, j) + (s(2, j) \cdot (i - 1))) \cdot \tan \alpha \quad (4)$$

where s represents the width of the zone (m).

Distance (m) from the mouth of the burner to the point of contact of two adjacent beams (L_1) and of contact of the edge beam with the wall (L_2):

$$L_1 = \frac{d(1,2)}{2 \cdot \tan \alpha} \quad L_2 = \frac{\frac{d(1,2)}{2} + d(1,1)}{\tan \alpha} \quad (5)$$

where d is the length of zone (m) and $\tan \alpha$ represents the tangent of the half angle at which the beam emerges from the burner (i.e., tangent of half beam angle).

The i -th index of the zones in which the contact is made is determined as follows:

$$d_1 = \text{int} \left(\frac{L_1 - 0.2}{s(1,2)} \right) \quad d_2 = \text{int} \left(\frac{L_2 - 0.2}{s(1,1)} \right) \quad (6)$$

The model takes into account the natural recirculation of flue gases. The following applies to the amount of flue gas from the burner orifice up to the contact of the beams with each other or with the wall (i.e., for $i = 1, \dots, d_1; j = 2, \dots, n - 1$):

$$Q_P(i, j, 3) = 0.32768 \cdot \frac{Q_0}{d_h} \cdot (s(1, j) + (s(2, j) \cdot (i - 1))) \quad (7)$$

The amount of flue gas sucked to these zones from the side surfaces is (i.e., for $k = 2, 4$):

$$Q_P(i, j, k) = \frac{(-Q_P(i, j, 3) - Q_P(i, j, 1))}{2} \quad (8)$$

Sucked amount of flue gas calculated according to equation (7), is returned by backward recirculation of the flue gas from the site $i = d_1 + 1$, for $j = 2, \dots, n - 1$. Recirculated volume amounts are defined by the equations (i.e., (9) for $j = 2, 4, \dots, n - 1$ and (10) for $j = 3, 5, \dots, n - 2$):

$$Q_P(d_1 + 1, j, k) = \sum_{i=1}^{d_1} Q_P(i, j, 4) \quad (9)$$

$$Q_P(d_1 + 1, j, k) = \sum_{i=1}^{d_1} Q_P(i, j, 2) \quad (10)$$

The recirculation of flue gas volume flows for zones $s_j = 1, j = n$, and $i = d_1 + 1, \dots, d_2$ can be determined analogously to equations (9), (10) for zones $s_j = 1, j = n$, and $i = d_1 + 1, \dots, d_2$ taking into account their recirculation from individual zones according to the proportions calculated according to equation (11) (i.e., for $i = d_1 + 1, \dots, d_2; j = 2, \dots, n - 1$):

$$P(i, j) = \frac{r(i, j) - \frac{d(i, j)}{2}}{\sum_{i=d_1+1}^{d_2} r(i, j) - \frac{d(i, j)}{2}} \quad (11)$$

where P is the contribution of the part of the exhausted flue gases belonging to the i -th zone.

$$Q_P(i, 1, 4) = P(i, 1) \cdot \sum_{i=1}^{d_1} Q_P(i, 2, 2) \quad (12)$$

$$Q_P(i, 1, 1) = Q_P(i, 2, 2) + Q_P(i - 1, 1, 3) \quad (13)$$

where (9) is for $i = d_1 + 1, \dots, d_2$ and (10) is for $i = 2, \dots, d_1$.

The total amount of fuel and combustion air mixture exiting the burner:

$$Q_{burner} = Q_{fuel} + Q_{air} = Q_{fuel} + Q_{air_min} \cdot \beta \quad (14)$$

where Q_{fuel} is the fuel amount (m^3/s), Q_{air} is the combustion air amount (m^3/s), Q_{air_min} is the combustion air minimal amount (m^3/s), β is the excess air.

The excess air β is set in the range 1 - 1.1 (i.e., the optimal value for natural gas combustion).

The amount Q_{fuel} is increased by recirculated flue gas in the individual zones:

$$Q_{flue_gas} = Q_{burner} + Q_{recirc} \quad (15)$$

where Q_{recirc} is the amount of recirculated flue gas (m^3/s).

The amount of recirculated flue gas Q_{recirc} is within limits (0; Q_{burner}). The law of conservation of fluids momentum applies to the whole combustion space and each zone:

$$p_{flue_gas} = m_{flue_gas} \cdot w_{flue_gas} \quad (16)$$

where m_{flue_gas} is the weight of flue gas (kg) and w_{flue_gas} is the velocity of flue gas (w/s).

The maximum burner outlet velocity w_{flue_gas} is 40 cm/s. The total amount of flue gas exhausted is increased about the total amount of recirculated flue gas. The count of burners is taken into account in this balance:

$$Q_{flue_gas,exhausts} = \sum_{burner} Q_{burner} + \sum_{burner} Q_{recirc} \quad (17)$$

RESULTS AND DISCUSSIONS

The so-called piston flow is valid for zones from the point of contact to the flue gas draught zones, or to the point of collision of opposing streams. The condition of the overall material balance must be observed for flue gas draught. The model will reveal critical parts of the furnace space, where there is a presumption of a sudden increase in temperature or its decrease, which may negatively affect the life of the lining during the operation of the combustion aggregate. It is not the task of examining the exact distribution of the temperature field in the entire furnace space or the precise determination of the concentration of individual components in the flue gas. But it can identify places where this flue gas composition needs to be determined with a higher frequency. The user can adjust the density of the zonal network according to needs. It can also change the fuel consumption in individual burners according to the technological mode of combustion in the furnace.

The volume zones were determined for the dimensions of the furnace 17 x 8.37 m and the total number of burners 13 + 13. The basic flue gas flow from the burner side was set to 0.02777 Nm^3/s (Table 1). This flow was adjusted to a

one-third value for the material output side (Table 2 and 3). In the simulation shown in Table 3, zero flow rates were set for every second burner located on the material inlet side. Based on equation (17), the following balance components are applied to the checking of volume flows in the working space of the furnace for the tested cases:

In the first case, the amount of flue gas $Q_{burner} = 27.77 \cdot 26 = 722.02 \text{ Ndm}^3/\text{s}$ is supplied to the inlets (i.e., burner side). The amount $Q_{flue_gas,exhausts} = 1301.9 \text{ Ndm}^3/\text{s}$ passes through three exhausts. The difference between inlets and exhausts is the recirculated amount (i.e., $579.88 \text{ Ndm}^3/\text{s}$). According to Table 1, the amount $Q_{recirc} = 4 \cdot (80.79 + 63.43) \text{ Ndm}^3/\text{s}$ is supplied evenly from the edge zones (i.e., $j = 1$ and $j = 15$) from both burner sides. The calculated values for the second case are $Q_{burner} = 13 \cdot 27.77 + 13 \cdot 27.77/3 = 481.35 \text{ Ndm}^3/\text{s}$ and $Q_{flue_gas,exhausts} = 679.6 \text{ Ndm}^3/\text{s}$. The calculated values for the third case are $Q_{burner} = 7 \cdot 27.77 + 13 \cdot 27.77/3 = 314.73 \text{ Ndm}^3/\text{s}$ and $Q_{flue_gas,exhausts} = 509.2 \text{ Ndm}^3/\text{s}$. The recirculated amount Q_{recirc} is $198 \text{ Ndm}^3/\text{s}$ for the second case and $195 \text{ Ndm}^3/\text{s}$ for the third case. The recirculated amount's reduction corresponds to reducing the flue gas flow through the burners on the material inlet side to the furnace.

The most thermally stressed zones are at the meeting point of the adjacent flames (i.e., $i = 5, 6$).

The least flue gas occurs in the area (i.e., $i = 9, 10$). It can also be seen in Figure 3, before the redistribution of flows into the exhaust zones, i.e., the zones highlighted in the tables (i.e., 13, 4; 13, 8; 13, 12). Since the exhausts (i.e., gas draughts) are located more on the material outlet side, this is not so pronounced with these burners. The encounter of opposing flames is in the zones (i.e., $i = 12, 13, 14$), but it is markedly visible only at the walls of the furnace because in other zones, the force of flue gas draught is manifested. Here it would be necessary to solve only the consequences of gas outflows from the furnace space. Alternating operating or redistributed adjacent burners will improve the redistribution of flue gases from zone $i = 6$, as the meeting point of adjacent flames will be moved closer to the exhaust zones. With a burner and exhaust system created in this way, it does not make sense to discard the entire burner side because only a small amount of flue gas would pass along the furnace walls, and by recirculation, it would not be possible to achieve a sufficient flue gas concentration and thus a sufficient temperature in the furnace space on the material outlet side.

The most thermally stressed parts of the refractory brickwork are in the area of meeting adjacent and opposite flue gas flows from the burners. Their location concerning the burner outlet diameter does not change, and the amount of flue gas present

Table 1. Redistribution of flue gas flow in i,j volume zones for uniform flow of burners

Flue gas flow (Ndm ³ /s)															
i\j	15	14	13	12	11	10	9	8	7	6	5	4	3	2	1
1	11.33	50.42	50.42	50.42	50.42	50.42	50.42	50.42	50.42	50.42	50.42	50.42	50.42	50.42	11.33
2	28.69	85.16	85.16	85.16	85.16	85.16	85.16	85.16	85.16	85.16	85.16	85.16	85.16	85.16	28.69
3	46.06	119.89	119.89	119.89	119.89	119.89	119.89	119.89	119.89	119.89	119.89	119.89	119.89	119.89	46.06
4	63.43	154.62	154.62	154.62	154.62	154.62	154.62	154.62	154.62	154.62	154.62	154.62	154.62	154.62	63.43
5	80.79	189.36	189.36	189.36	189.36	189.36	189.36	189.36	189.36	189.36	189.36	189.36	189.36	189.36	80.79
6	80.79	189.36	189.36	189.36	189.36	189.36	189.36	189.36	189.36	189.36	189.36	189.36	189.36	189.36	80.79
7	67.38	162.53	162.53	162.53	162.53	162.53	162.53	162.53	162.53	162.53	162.53	162.53	162.53	162.53	67.38
8	40.56	108.89	108.89	108.89	108.89	108.89	108.89	108.89	108.89	108.89	108.89	108.89	108.89	108.89	40.56
9	6.41	28.42	56.83	113.67	28.42	28.42	56.83	142.08	56.83	28.42	28.42	113.67	56.83	28.42	6.41
10	6.41	28.42	56.83	198.91	28.42	28.42	56.83	255.75	56.83	28.42	28.42	198.91	56.83	28.42	6.41
11	40.56	108.89	108.89	198.91	108.89	108.89	108.89	255.75	108.89	108.89	108.89	198.91	108.89	108.89	40.56
12	67.38	162.53	162.53	198.91	162.53	162.53	162.53	255.75	162.53	162.53	162.53	198.91	162.53	162.53	67.38
13	80.79	189.36	189.36	415.09	189.36	189.36	189.36	471.93	189.36	189.36	189.36	415.09	189.36	189.36	80.79
14	80.79	189.36	189.36	189.36	189.36	189.36	189.36	189.36	189.36	189.36	189.36	189.36	189.36	189.36	80.79
15	63.43	154.62	154.62	154.62	154.62	154.62	154.62	154.62	154.62	154.62	154.62	154.62	154.62	154.62	63.43
16	46.06	119.89	119.89	119.89	119.89	119.89	119.89	119.89	119.89	119.89	119.89	119.89	119.89	119.89	46.06
17	28.69	85.16	85.16	85.16	85.16	85.16	85.16	85.16	85.16	85.16	85.16	85.16	85.16	85.16	28.69
18	11.33	50.42	50.42	50.42	50.42	50.42	50.42	50.42	50.42	50.42	50.42	50.42	50.42	50.42	11.33

there depends on the fuel flow to the burners and the recirculation. Regenerative burners should be applied to the most thermally stressed parts, in which the recirculation rate increases. The flue gas draught area, which is firmly located in specific

zones of the furnace space, can only be solved by changing the pressure conditions at the exhausting point. It is essential to maintain a stable flame for all these adjustments. It is related to the regulation of the flow rate of fuel and air in the given burners.

Table 2. Redistribution of flue gas flow in *i,j* volume zones for adjusted flow of burners

Flue gas flow (Ndm ³ /s)															
i\j	15	14	13	12	11	10	9	8	7	6	5	4	3	2	1
1	11.33	50.42	50.42	50.42	50.42	50.42	50.42	50.42	50.42	50.42	50.42	50.42	50.42	50.42	11.33
2	28.69	85.16	85.16	85.16	85.16	85.16	85.16	85.16	85.16	85.16	85.16	85.16	85.16	85.16	28.69
3	46.06	119.89	119.89	119.89	119.89	119.89	119.89	119.89	119.89	119.89	119.89	119.89	119.89	119.89	46.06
4	63.43	154.62	154.62	154.62	154.62	154.62	154.62	154.62	154.62	154.62	154.62	154.62	154.62	154.62	63.43
5	80.79	189.36	189.36	189.36	189.36	189.36	189.36	189.36	189.36	189.36	189.36	189.36	189.36	189.36	80.79
6	80.79	189.36	189.36	189.36	189.36	189.36	189.36	189.36	189.36	189.36	189.36	189.36	189.36	189.36	80.79
7	67.38	162.53	162.53	162.53	162.53	162.53	162.53	162.53	162.53	162.53	162.53	162.53	162.53	162.53	67.38
8	40.56	108.89	108.89	108.89	108.89	108.89	108.89	108.89	108.89	108.89	108.89	108.89	108.89	108.89	40.56
9	6.41	28.42	56.83	113.67	28.42	28.42	56.83	142.08	56.83	28.42	28.42	113.67	56.83	28.42	6.41
100	2.13	9.46	18.91	142.03	9.46	9.46	18.91	179.9	18.91	9.46	9.46	142.03	18.91	9.46	2.13
11	13.49	36.23	36.23	142.03	36.23	36.23	36.23	179.9	36.23	36.23	36.23	142.03	36.23	36.23	13.49
12	22.42	54.08	54.08	142.03	54.08	54.08	54.08	179.9	54.08	54.08	54.08	142.03	54.08	54.08	22.42
13	26.88	63	63	213.96	63	63	63	251.83	63	63	63	213.96	63	63	26.88
14	26.88	63	63	63	63	63	63	63	63	63	63	63	63	63	26.88
15	21.1	51.45	51.45	51.45	51.45	51.45	51.45	51.45	51.45	51.45	51.45	51.45	51.45	51.45	21.1
16	15.33	39.89	39.89	39.89	39.89	39.89	39.89	39.89	39.89	39.89	39.89	39.89	39.89	39.89	15.33
17	9.55	28.33	28.33	28.33	28.33	28.33	28.33	28.33	28.33	28.33	28.33	28.33	28.33	28.33	9.55
18	3.77	16.78	16.78	16.78	16.78	16.78	16.78	16.78	16.78	16.78	16.78	16.78	16.78	16.78	3.77

Table 3. Redistribution of flue gas flow in *i,j* volume zones for switching off burners from one side

Flue gas flow (Ndm ³ /s)															
i\j	15	14	13	12	11	10	9	8	7	6	5	4	3	2	1
1	11.33	50.42	50.42	50.42	50.42	50.42	50.42	50.42	50.42	50.42	50.42	50.42	50.42	50.42	11.33
2	28.69	85.16	85.16	85.16	85.16	85.16	85.16	85.16	85.16	85.16	85.16	85.16	85.16	85.16	28.69
3	46.06	119.89	119.89	119.89	119.89	119.89	119.89	119.89	119.89	119.89	119.89	119.89	119.89	119.89	46.06
4	63.43	154.62	154.62	154.62	154.62	154.62	154.62	154.62	154.62	154.62	154.62	154.62	154.62	154.62	63.43
5	80.79	189.36	189.36	189.36	189.36	189.36	189.36	189.36	189.36	189.36	189.36	189.36	189.36	189.36	80.79
6	80.79	189.36	189.36	189.36	189.36	189.36	189.36	189.36	189.36	189.36	189.36	189.36	189.36	189.36	80.79
7	67.38	162.53	162.53	162.53	162.53	162.53	162.53	162.53	162.53	162.53	162.53	162.53	162.53	162.53	67.38
8	40.56	108.89	108.89	108.89	108.89	108.89	108.89	108.89	108.89	108.89	108.89	108.89	108.89	108.89	40.56
9	6.41	28.42	56.83	113.67	28.42	28.42	56.83	142.08	56.83	28.42	28.42	113.67	56.83	28.42	6.41
100	2.13	9.46	18.91	142.03	9.46	9.46	18.91	179.9	18.91	9.46	9.46	142.03	18.91	9.46	2.13
11	13.49	36.23	36.23	142.03	36.23	36.23	36.23	179.9	36.23	36.23	36.23	142.03	36.23	36.23	13.49
12	22.42	54.08	54.08	142.03	54.08	54.08	54.08	179.9	54.08	54.08	54.08	142.03	54.08	54.08	22.42
13	26.88	63	63	213.96	63	63	63	251.83	63	63	63	213.96	63	63	26.88
14	26.88	63	63	63	63	63	63	63	63	63	63	63	63	63	26.88
15	21.1	51.45	51.45	51.45	51.45	51.45	51.45	51.45	51.45	51.45	51.45	51.45	51.45	51.45	21.1
16	15.33	39.89	39.89	39.89	39.89	39.89	39.89	39.89	39.89	39.89	39.89	39.89	39.89	39.89	15.33
17	9.55	28.33	28.33	28.33	28.33	28.33	28.33	28.33	28.33	28.33	28.33	28.33	28.33	28.33	9.55
18	3.77	16.78	16.78	16.78	16.78	16.78	16.78	16.78	16.78	16.78	16.78	16.78	16.78	16.78	3.77

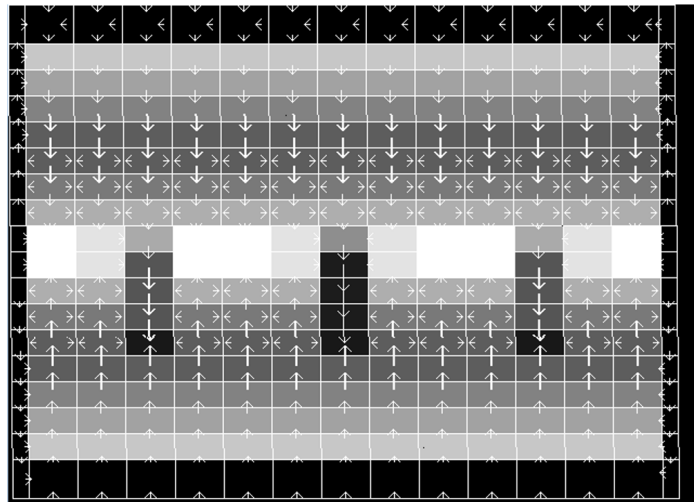


Fig. 3. Redistribution of flue gas flows to furnace volume zones for uniform flow through burners

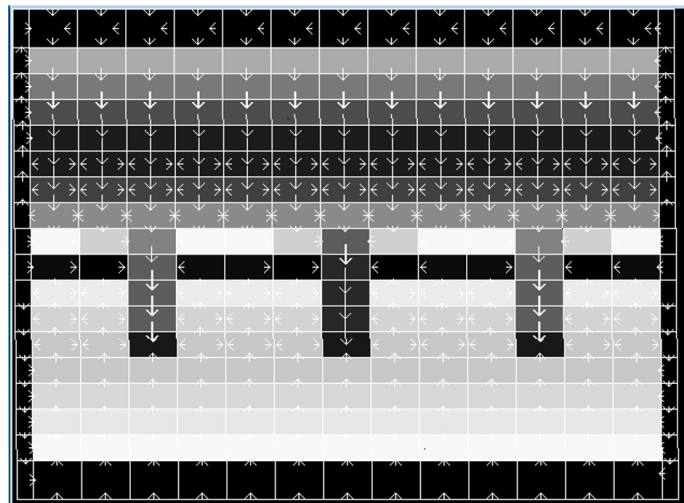


Fig. 4. Redistribution of flue gas flows to furnace volume zones for adjusted flow through burners

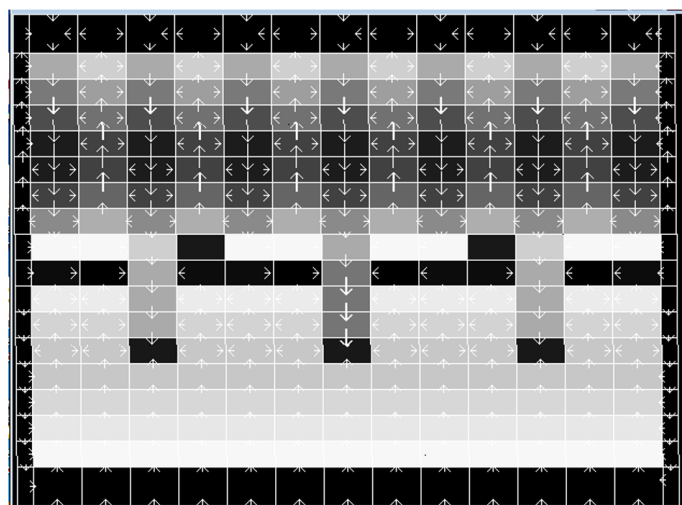


Fig. 5. Redistribution of flue gas flows to furnace volume zones for switching off burners from one side

CONCLUSION

The created model is based on zonal flow conditions concerning the material balance and maintaining the stability of combustion in the furnace space. This model allows the variable setting of the qualitative and quantitative properties of the fuel and geometric characteristics of the furnace. The paper describes three selected simulated cases (see Tab. 1-3 and Fig. 3-5). The individual cases differed by the setting of the inlet flow to the burner zones, which also enables a simulated burner switch-off or change in its characteristics. Based on the achieved simulation results, the following conclusions can be generalized.

The most thermally stressed zones are at the point where the adjacent flames meet and when the flows from the edge burners collide with the furnace walls. Reducing the flow to the burners at the material inlet to the furnace reduced the recirculated amount from 579 Ndm³/s to 198 Ndm³/s. This reduction affected internal recirculation (i.e., in the the processed material space) and recirculation at the furnace walls. Subsequently, switching off the burners at the furnace outlet did not significantly affect the overall recirculation, i.e., the decrease of the recirculated amount from 198 Ndm³/s to 195 Ndm³/s. This reduction did not have a significant effect on the thermal stress of the furnace walls. The obtained results showed that a change in the operating mode of the burners (e.g., change of flow value) at the material inlet into the furnace significantly affects the recycled amount (i.e., heat transfer in the furnace working space) as opposed to a change in the burners operating mode (i.e., burner on-off) at furnace exit.

The least flue gas occurs before the redistribution of flows to the exhaust zones. The amount of flue gas occurred in the zones depends on the fuel flow to the burners and the recirculation or enthalpy changes of the flue gas in the individual volume zones. In the case of thermally stressed parts of the refractory brickwork, it is possible to replace conventional burners with regenerative burners; in these cases, the share of waste gas recirculation increases.

The exhaust area can be solved by changing the local pressure conditions or by regulating the exhaust fan located in the common flue. For all these modifications, it is important to maintain a stable flame distribution in the furnace space, which is closely related to the regulation of the flow rate and quality of fuel and air in the respective burners.

The created model is adaptable to the required conditions of the user, who determines the density of the network of volume zones determining the direction of flue gas flow in the working space of the furnace. The results obtained by the model showed the places with the highest heat load for the batch and the lining. This allows proposals for the reconstruction of the existing burner system and possible overall structural modification of the furnace. The proposed model can be used to determine the input parameters in the form of a heat flows matrix for models determining the temperatures inside the heated material and the hearth lining. These obtained data can then be used in the optimal technological control of heating furnaces.

Acknowledgments

This work was supported by the Slovak Grant Agency for Science under grants VEGA 1/0277/21, VEGA 1/0182/21, and by the Slovak Research and Development Agency under contract No. APVV-18-0526 and APVV-14-0892.

REFERENCES

- Hassan, A. A., Hamed, M.S. Modeling of Heat Treatment of Randomly Distributed Loads in Multi-Zone Continuous Furnaces. *Materials Science Forum*, 706-709, 2012, 289-294, 10.4028/www.scientific.net/MSF.706-709.289.
- Honner, M., Vesely, Z., Svantner, M. Temperature and heat transfer measurement in continuous reheating furnaces. *Scandinavian Journal of Metallurgy*, 32 (5), 2003, 225-232, 10.1034/j.1600-0692.2003.00645.x.
- Kang, J.W., Huang, T.Y., Purushothaman, R., Wang, W.W., Rong, Y.M. Modeling and simulation of heat transfer in loaded continuous heat treatment furnace. *14th Congress of International Federation for heat Treatment and Surface Engineering*, Vols 1 and 2, Proceedings, 2004, 764-768.
- Rad, S.D., Ashrafzadeh, A., Nickaen, M. Numerical simulation of fluid flow and heat transfer in an industrial continuous furnace. *Applied Thermal Engineering*, 2017, 2017, 263-274, 10.1016/j.apthermaleng.2017.02.031.
- Fuyong S., Heating and Flow Analysis in Hot-Rolled Stainless Strip Continuous Annealing Furnace Based on CFD Modeling, *Heat Transfer—Asian Research*, 46 (7), 2017, 924-932, 10.1002/htj.21251.
- Zhou, G., Wen, Z., Dou, R. F., Su, F.Y., Fang, X., Zhuang, W.Q., Cao, Y. The Steady-state Model of

- Heating Process in Horizontal Continuous Annealing Furnace. *Fundamental of Chemical Engineering*, 233-235, 2011, 2428-2431, 10.4028/www.scientific.net/AMR.233-235.2428.
7. Sahay, S. S., Kapur, P.C. Model based scheduling of a continuous annealing furnace. *Ironmaking & Steelmaking*, 34 (3), 2007, 262-268, 10.1179/174328107X165708.
 8. Zhang, C., Qin, J., Yang, Q., Zhang, S., Chang, J., Bao, W. Indirect measurement method of inner wall temperature of scramjet with a state observer. *Acta Astronautica*, 115, 2015, 330-337, 10.1016/j.actastro.2015.05.030.
 9. Sahay, S. S., Krishnan, K. Model based optimization of continuous annealing operation for bundle of packed rods. *Ironmaking & Steelmaking*, 34 (1), 2007, 89-94, 10.1179/174328106X118170.
 10. Steinboeck, A., Wild, D., Kugi, A. Feedback Tracking Control of Continuous Reheating Furnaces. *Proceedings of the 18th World Congress the International Federation of Automatic Control*, 44 (1), 2011, 11744-11749, 10.3182/20110828-6-IT-1002.01639.
 11. Wild, D., Meurer, T., Kugi, A. Modelling and experimental model validation for a pusher-type reheating furnace. *Mathematical and Computer Modelling of Dynamical Systems*, 15 (3), 2009, 209–232, 10.1080/13873950902927683.
 12. Hajaliakbari, N., Hassanpour, S. Analysis of thermal energy performance in continuous annealing furnace. *Applied Energy*, 206, 2017, 829–842, 10.1016/j.apenergy.2017.08.246.
 13. Goyheneche, J. M., Sacadura, J. F. The Zone Method: A New Explicit Matrix Relation to Calculate the Total Exchange Areas in Anisotropically Scattering Medium Bounded by Anisotropically Reflecting Walls. *Journal of Heat Transfer, Transactions of the ASME*, 124, 2002, 696-703, 10.1115/1.1481359.
 14. Hu, W., Jia, P., Nie, J., Gao, Y. and Zhang, Q. A Fast Prediction Model for Heat Transfer of Hot-Wall Heat Exchanger Based on Analytical Solution. *Applied Science*, 9 (72), 2019, 1-18, 10.3390/app9010072.
 15. Hu, G., Zhang, Y., Du, W., Long, J., Qian, F. Zone method based coupled simulation of industrial steam cracking Furnaces. *Energy*, 172, 2019, 1098-1116, 10.1016/j.energy.2018.12.190.
 16. Xiang, L., Song, E., Ding, Y. A Two-Zone Combustion Model for Knocking Prediction of Marine Natural Gas SI Engines. *Energies*, 11 (3), 2018, 1-23, 10.3390/en11030561.
 17. Kreuzer, D. R., Werner, A. Implementation of Models for reheating processes in industrial furnaces, *Proceedings 8th Modelica Conference*, 2011, 376-387.
 18. Kaprielian, L., Demoulin, M., Cinnella, P., Daru V. Multi-Zone Quasi-Dimensional Combustion Models for Spark-Ignition Engines. *Conference: 11th International Conference on Engines & Vehicles*, Volume: SAE Technical Paper Series 2013-24-0025, 2013, 10.4271/2013-24-0025.
 19. Li, R. C., Zhu, G. G. A Control-Oriented Reaction-Based SI Engine Combustion Model. *Proceedings of the ASME 2018 Dynamic Systems and Control Conference*, 2018, DSCC2018-8988, 1-8, 10.1115/DSCC2018-8988.
 20. Oba, R., Possamai, T.S., Nunes, A.T., Nicolau, V.P. Numerical simulation of tunnel kilns applied to white tile with natural gas. *Proceedings of COBEM 2011 21st Brazilian Congress of Mechanical Engineering*, 2011.
 21. Shiehnejadhesar, A., Mehrabian, R., Scharler, R., Goldin, G. M., Obernberger, I. Development of a gas phase combustion model suitable for low and high turbulence conditions, *Fuel*, 126 (15), 2014, 177-187, 10.1016/j.fuel.2014.02.040.
 22. Zhang, C., Usmani, A. Heat transfer principles in the thermal calculation of structures in fire, *Fire Safety Journal*, 78, 2015, 85–95, 10.1016/j.fire-saf.2015.08.006.
 23. Lukáč, L., Kizek, J., Jablonský, G., Karakash, Y. Defining the Mathematical Dependencies of NOx and CO Emission Generation after Biomass Combustion in Low-Power Boiler, *Civil and Environmental Engineering Reports*, 29 (3), 2019, 153-163, 10.2478/ceer-2019-0031.
 24. Drábikova, E., Škrabuláková, E. F. Reducing costs by graph algorithms. *19th International Carpathian Control Conference*, 2018, 113 – 117, 10.1109/carpathiancc.2018.8399612.
 25. Škrabuláková, E. F., Grešová, E. Cost Saving via Graph Coloring Approach. *Scientific Papers of the University of Pardubice: Series D*, 27 (45), 2019, 152-160, ISSN 1211-555X.